***IN SITU* DETERMINATION OF SIDEROPHILE TRACE ELEMENTS IN METALS AND SULFIDES IN ENSTATITE ACHONDRITES.** D. van Acken[1] , M. Humayun[2], A.D. Brandon[3], and A. Peslier[1,4] [1]NASA-JSC, 2101 NASA Parkway, MS KR, Houston, TX 77058, USA (david.vanacken@nasa.gov), [2]National High Magnetic Field Laboratory and Dept. of Geological Sciences, Florida State University, Tallahassee, FL 32310, USA (humayun@magnet.fsu.edu), [3]University of Houston, Dept. of Earth and Atmospheric Sciences, Houston, TX 77204 (abrandon@uh.edu), [4]Jacobs Technology, E.S.C.G., Mail Code JE23, 2224 Bay Area Blvd, Houston, TX 77058, USA (anne.h.peslier@nasa.gov).

Introduction: Enstatite meteorites are identified by their extremely reduced mineralogy (1) and similar oxygen isotope composition (2). The enstatite meteorite clan incorporates both EH and EL chondrites, as well as a wide variety of enstatite achondrites, such as aubrites or anomalous enstatite meteorites (e.g. Mt. Egerton, Shallowater, Zakłodzie, NWA 2526). The role of nebular versus planetary processes in the formation of enstatite meteorites is still under debate (e.g. 3-5). Past studies showed a significant influence of metal segregation in the formation of enstatite achondrites. Casanova et al. (6) suggested incomplete metal-silicate segregation during core formation and attributed the unfractionated siderophile element patterns in aubrites metals to a lack of fractional crystallization in a planetary core. Recent studies suggest a significant role of impact melting in the formation of primitive enstatite chondrites (7) and identified NWA 2526 as a partial melt residue of an enstatite chondrite (8). To understand the nature of siderophile element-bearing phases in enstatite achondrites, establish links between enstatite achondrites and enstatite chondrites (9), and constrain planetary differentiation on their respective parent bodies and their petrogenetic histories, we present laser ablation ICP-MS measurements of metal and sulfide phases in Shallowater, Mt. Egerton, and the aubrites Aubres, Cumberland Falls, and Mayo Belwa.

Samples and Analytical Methods: Thin sections were obtained from the Smithsonian Institution, and examined for major element composition using the Cameca SX100 electron microprobe at NASA-Johnson Space Center (JSC). Laser ablation ICP-MS analyses were performed at NHMFL at Florida State University, using a New Wave UP193 FX laser ablation system attached to a Thermo Element XR. Depending on grain size, grains were either analyzed with a 50 µm line scan, 10 µm/s scan speed, or as single spots with beam diameter adjusted to grain size (between 50 and 100 µm), 2 seconds dwell time. All measurements used 20 Hz repetition rate, at 100% power output (2.4 GW/cm^2, 11 J/cm^2). Analyzed peaks were ^{23}Na, ^{25}Mg, ^{27}Al, ^{29}Si, ^{31}P, ^{34}S, ^{39}K, ^{44}Ca, ^{45}Sc, ^{47}Ti, ^{51}V, ^{53}Cr, ^{55}Mn, ^{57}Fe, ^{59}Co, ^{60}Ni, ^{63}Cu, ^{66}Zn, ^{69}Ga, ^{74}Ge, ^{77}Se, ^{88}Sr, ^{89}Y, ^{90}Zr, ^{93}Nb, ^{97}Mo, ^{102}Ru, ^{103}Rh, ^{106}Pd, ^{120}Sn, ^{121}Sb, ^{125}Te, ^{184}W, ^{185}Re, ^{192}Os, ^{193}Ir, ^{195}Pt, and ^{197}Au, in low resolution mode. Standards used were North Chile (Filomena) IIA and Hoba IVB iron meteorites, NIST 1263a steel, MPI-DING basaltic glasses, and pyrite single crystals.

Results: *Shallowater:* The major siderophile element bearing phases is troilite (FeS) with minor metal inclusions not detectable by microprobe. Troilite is homogeneous in terms of major element composition, with ~0.15 wt% Ni, 0.65 – 0.70 wt% Ti, 0.35 – 0.40 wt% Mn and 3.50 – 3.75 wt% Cr as notable minor elements. Up to 9% bulk metal content have been reported for other sections of Shallowater (5), however, such large contents were not observed in our section (USNM 1206 #2). Shallowater troilite is enriched in Cu, Mo and Re, and poor in Os, Ir, Pd and Ga (Fig.1a), with a non-chondritic siderophile element pattern.

Mt. Egerton: Microprobe analysis of large metal grains, several mm to cm in size, show a fairly homogeneous major element distribution, with Ni contents between 4 and 8 wt% and Si contents about 1.8 – 2.0 wt%. Traverses across large metal grains reveal small P-rich domains (schreibersite), which show enrichment in Co, Mo, and Ru. Metal samples have a siderophile element pattern broadly similar to enstatite chondrites (10), with depletions in Cu and Sn, and enrichments in Co and Au compared to CI chondrites (Fig. 1b). One grain shows low Os, Ir, As, and Au.

Aubrites sensu stricto (Cumberland Falls, Mayo Belwa, Aubres): The analyzed aubrite sections contain a number of sulfides along with small amounts of metal which is typical for enstatite meteorites,. Siderophile element behavior is controlled by these small metal grains. One grain from Mayo Belwa shows almost no fractionation compared to chondritic values, except for depletion in volatile siderophiles. Two metal grains from Aubres are strongly depleted in Re, Os, Ir, Pt, and Cu, with otherwise largely flat patterns. Cumberland Falls displays large internal heterogeneity. Patterns are fairly uniform for the more volatile elements, but show different degrees of depletion in compatible Re, Os, Ir, Pt (Fig.2).

Discussion: Formation models for the aubrites studied here include an origin from nebular condensation (3), restites from partial melting of an enstatite chondritic parent body (9, 11), or an origin as cumulates

from fractional crystallization (1, 5). The observed siderophile element patterns are difficult to reconcile with an origin of metal and sulfides in enstatite achondrites from nebular condensation (3), because their fractionation patterns clearly indicate that parent body processes (partial melting and fractional crystallization) played the dominant role in controlling compatible siderophile element abundances.

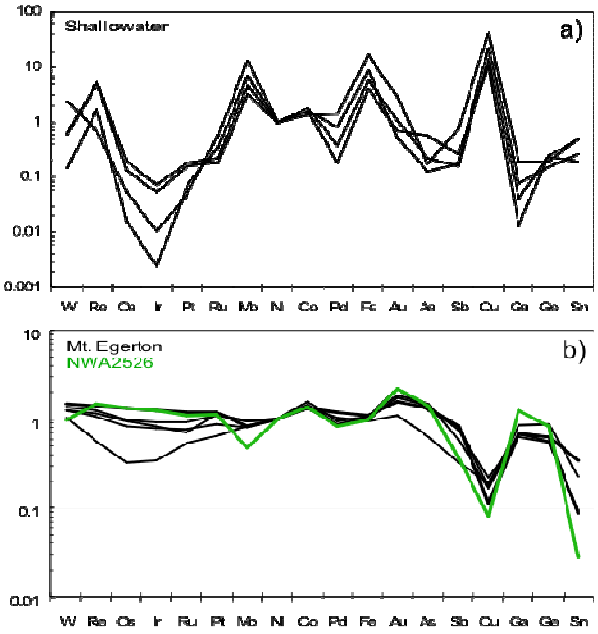

Fig. 1: CI chondrite-, Ni- normalized elemental concentrations for (a) Shallowater troilite and (b) Mt. Egerton metal; green line: NWA2526 from (8)

In contrast to the findings of (6), we found significant fractionation of siderophile elements in Mt. Egerton metal, as well as in Aubres and Cumberland Falls. The depletion of compatible Re, Os, Ir and Pt in these samples indicates formation from liquid metal, either by the quenching of small amounts of metallic liquid, or by crystallization of solid metal from a partial melt. This depletion, as observed in Aubres and Cumberland Falls, is inconsistent with an origin as restites from partial melting, and contrasts with the siderophile element pattern observed in a restitic enstatite meteorite, NWA 2526 (8). Similar patterns in the EL3 chondrite PCA 91020 have been interpreted as a signature of metal liquid produced by impact melting (7). The presence of metal grains exhibiting a wide range of Os/Ni, Ir/Ni, etc., in Cumberland Falls (Fig. 2a) implies that its metal underwent fractionation crystallization probably within the magma chamber in which the various clasts evolved. Mt. Egerton patterns are similar to the NWA 2526 pattern (Fig. 1b), except for the absence of the Mo depletion, probably due to lower sulfide in the Mt. Egerton magma, and depletions of compatible Re, Os, Ir, indicating that Mt. Egerton metal could have formed from a high degree partial melt.

For Shallowater, the situation is currently less clear since no metal was available for analysis. An igneous origin on a different parent body along with a complex cooling history was suggested by (5). The observed sulfide patterns show potential loss of a refractory-enriched metal component, while the trends defined by the more volatile elements indicate a common origin with the aubrites (Fig. 1, 2). The ubiquitous presence of high W/Ir and Re/Os ratios in metal from enstatite achondrites is consistent with high carbon content in the metallic liquid (12).

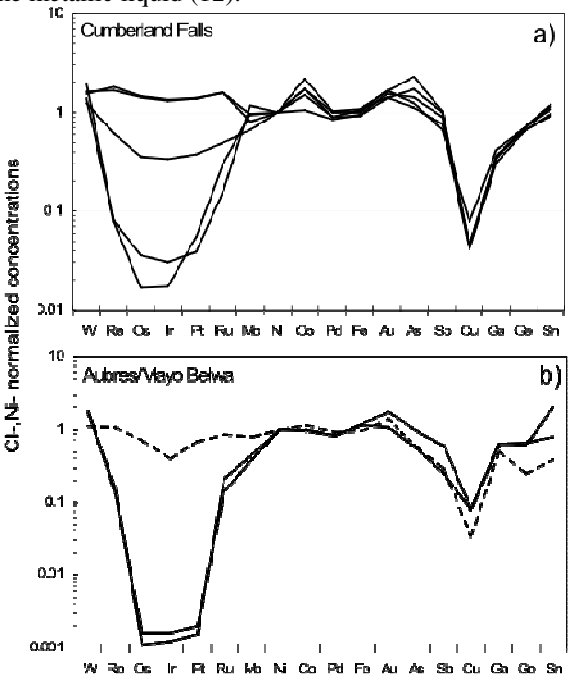

Fig. 2 CI chondrite-, Ni- normalized elemental concentrations for metal in (a) Cumberland Falls and (b) Aubres (solid) and Mayo Belwa (dashed)

References: [1] Keil K. (1989) *Meteoritics, 24,* 195-208. [2] Clayton R.N. et al. (1984) *LPS XV,* C245-C249. [3] Wasson J.T. and Wai C.M. (1970) *GCA, 34,* 169-184. [4] Wolf R. et al (1983) *GCA, 47,* 2257–2270. [5] Keil K. et al (1989) *GCA, 53,* 3291- 3307. [6] Casanova I. et al (1993) *GCA, 57,* 675- 882. [7] van Niekerk D. et al (2009) *LPS XL,* Abstract #2049. [8] Humayun M. et al (2009) *LPS XL,* Abstract #1744. [9] Watters T.R. and Prinz M. (1979) *LPS X,* 1073-1093. [10] Hertogen J. et al (1983) *GCA, 47,* 2241–2255. [11] Fogel R.A. et al (1988) *LPS XIX,* 342-343. [12] Chabot N.L. et al (2006) *GCA, 70,* 1322-1335.